

UNCLASSIFIED

AD 414410

DEFENSE DOCUMENTATION CENTER

FOR

SCIENTIFIC AND TECHNICAL INFORMATION

CAMERON STATION, ALEXANDRIA, VIRGINIA



UNCLASSIFIED

NOTICE: When government or other drawings, specifications or other data are used for any purpose other than in connection with a definitely related government procurement operation, the U. S. Government thereby incurs no responsibility, nor any obligation whatsoever; and the fact that the Government may have formulated, furnished, or in any way supplied the said drawings, specifications, or other data is not to be regarded by implication or otherwise as in any manner licensing the holder or any other person or corporation, or conveying any rights or permission to manufacture, use or sell any patented invention that may in any way be related thereto.

414410

CATALOGED BY RFA

414410

**Electrical Engineering Research Laboratory
The University of Texas**

Austin, Texas

QUARTERLY ENGINEERING REPORT NO. 5

PART II

**ATMOSPHERIC ABSORPTION OF ELECTROMAGNETIC
RADIATION**

IN THE FREQUENCY RANGE 120 TO 132 KMC/S

by

C. O. Hemmi

Contract AF 33(657)-8716

Project 4062

**Aeronautical Systems Division
AIR FORCE SYSTEMS COMMAND
Wright-Patterson Air Force Base, Ohio**

**ELECTRICAL ENGINEERING RESEARCH LABORATORY
THE UNIVERSITY OF TEXAS
Austin, Texas**

QUARTERLY ENGINEERING REPORT NO. 5

PART II

**ATMOSPHERIC ABSORPTION OF ELECTROMAGNETIC RADIATION
IN THE FREQUENCY REGION 120 TO 132 KMC/S**

by

C. O. Hemmi

**Contract AF 33(657)-8716
Project 4062**

**Aeronautical Systems Division
AIR FORCE SYSTEMS COMMAND
Wright-Patterson Air Force Base, Ohio**

PART II

TABLE OF CONTENTS

	Page
LIST OF FIGURES	iii
ABSTRACT	iv
I. INTRODUCTION	1
II. SPECTROSCOPIC MEASUREMENTS AT MILLIMETER WAVELENGTHS	6
III. INSTRUMENTATION	8
IV. MEASUREMENT PROCEDURES	15
A. Atmospheric Measurements	15
B. Absorption Cell Measurements	18
V. RESULTS	23
VI. DISCUSSION	33
VII. CONCLUSIONS	38
BIBLIOGRAPHY	39

PART II

LIST OF FIGURES

No.		Page
1	Transmitter and receiver block diagrams	9
2	Photograph of transmitter	10
3	Photograph of receiving equipment	11
4	Photograph of transmitting bus	16
5	Photograph of absorption cell	19
6	Typical recordings	21
7	Measured values of atmospheric attenuation versus pressure for 2% water vapor molecular density	24
8	Attenuation versus water vapor density at 120 kMc/s for pressures of 737 and 462 millimeters of mercury	27
9	Attenuation versus water vapor density at 125 kMc/s for pressures of 737 and 462 millimeters of mercury	28
10	Attenuation versus water vapor density at 132 kMc/s for pressures of 737 and 462 millimeters of mercury	29
11	Dry air attenuation versus pressure at 120 kMc/s	30
12	Water vapor attenuation versus pressure for 2% water vapor molecular density	31
13	Water vapor attenuation versus pressure for a constant water vapor density of one gram per cubic meter	32
14	Calculated attenuation versus pressure for constant molecular density in the region of an absorption line	35
15	Measured values of water vapor attenuation and calculated oxygen and water vapor attenuation	37

PART II

ABSTRACT

The measurements and interpretation of the absorption of electromagnetic radiation by the earth's atmosphere at frequencies of 120, 125, and 132 kMc/s are described in this report. Data was taken at 5 pressures corresponding to pressure altitudes in the earth's atmosphere between 8 and 0.25 km. These measurements indicate the presence of a water vapor absorption line near 121 kMc/s with a peak intensity of 0.107 db/km gm/m³. The anomalous values of water vapor absorption observed by previous investigators may, therefore, be due to other unpredicted water vapor lines. Measurement techniques are described and previous measurements of water vapor attenuation are summarized.

I. INTRODUCTION

The absorption of microwave radiation by gases is one of the many types of interactions of electromagnetic radiation with matter. An analysis of these interactions usually involves quantum mechanics. From a quantum mechanical analysis of atoms and molecules, the allowed values of the total energy of the system can be determined. The analysis also shows that certain transitions between the allowed energy levels are permitted while others are not. These permitted transitions may involve radiation. The frequency of the radiation is related to the change in energy by $\Delta E = h \nu$; where ΔE is the change in energy, h is Planck's constant, and ν is the frequency. An energy transition by which radiation is absorbed results in an increase in energy of the atom or molecule and, since a very narrow band of frequencies is often involved in these energy transitions, the term absorption line is used to denote this phenomenon. The study of absorption and emission of microwave radiation by matter is known as microwave spectroscopy.

The transitions of electrons between electronic energy states result in relatively large energy changes and are associated with radiation in the optical region, while relative vibration of the atoms in a molecule is associated with radiation in the infrared region. The absorption of microwaves yields relatively small energy changes and requires closely spaced energy levels. These closely spaced levels are found in the rotational motion of the molecules of a gas. ^{9(a)} A permanent electric or magnetic dipole moment

provides the mechanism by which the radiation fields are coupled to the rotational motion of the molecule. ^{9(b)}

There are a number of effects that perturb the allowed energies of a molecular system and result in a broadening of the range of frequencies over which absorption can occur. There is a natural line width associated with an absorption which is the result of the disturbance of molecular energy levels by the zero-point fields which are always present in space. Doppler broadening is due to motion of the absorbing molecule relative to the direction of radiation, causing a shift in the frequency seen by the molecule. ^{9(c)} Saturation broadening results when the radiation is so intense that the relaxation mechanism for dissipating the energy absorbed by the molecules is not adequate and the energy distribution of the gas is significantly modified. This reduces the absorption at the line center relative to the absorption on either side of the line center and gives a broadening effect. ^{9(d)}

Collisions between molecules also perturb the energy levels of the molecules in a gas and result in broadening of absorption lines. It is the most important source of broadening of microwave lines in gases at atmospheric pressures equivalent to elevations between sea level and approximately 200,000 feet. A number of theories of collision broadening have been formulated. The most widely used has been that of Van Vleck and Weisskopf. ¹³ Their derivation considers a group of harmonic oscillators whose oscillations are interrupted momentarily at random times. The results of this classical analysis are identical with the results of quantum derivations. ^{3(a)} Classical

solutions also yield good approximations of the line resonant frequencies when the energy level transitions are small and the time duration of transitions are relatively long, such as those in the microwave frequency range. ^{14(a)}

According to the Van Vleck-Weisskopf formulation, the absorption coefficient of an isolated molecular line is given by ^{8(a)}

$$\gamma = 10^6 (\log_{10} e) \left(\frac{8\pi^2 \nu N}{6ckT} \right) \frac{|\mu_{ij}|^2 \nu_{ij} f(\nu_{ij}, \nu) e^{-E_i/kT}}{G} \quad (1)$$

where γ = absorption coefficient in decibels per kilometer

$|\mu_{ij}|^2$ = the line intensity of the i-j transition

c = the speed of light

T = absolute temperature

k = Boltzmann's constant

N = number of absorbing molecules per cubic centimeter

G = gas rotational energy partition function of the absorbing gas (dimensionless)

$e^{-E_i/kT}$ = fraction of molecules in a particular resonant energy level

$f(\nu_{ij}, \nu)$ = the shape factor

$$= \frac{1}{\pi} \frac{\nu}{\nu_{ij}} \left(\frac{\Delta \nu}{(\nu - \nu_{ij})^2 + \Delta \nu^2} + \frac{\Delta \nu}{(\nu + \nu_{ij})^2 + \Delta \nu^2} \right)$$

where $\Delta \nu$ = absorption line half-intensity half-width

ν_{ij} = the center frequency of the i-j transition.

The equation applies for molecules with either electric or magnetic dipole moments.

Of the gases found in the atmosphere, oxygen has a permanent magnetic moment while water vapor has an electric dipole moment. There are a number of other gases present in the atmosphere in small quantities that contribute to the absorption of microwaves but their effect is small.

The absorption due to magnetic moments is much smaller than that due to electric moments but in the case of atmospheric oxygen there are a large number of allowed transitions with resonant frequencies centered around 60 kMc/s and the combined effect of the absorption produced by these transitions results in relatively large values of atmospheric opacity. Oxygen also has a single isolated line at 118.75 kMc/s which becomes important when long transmission paths in the atmosphere are considered. Associated with the resonant absorption is a nonresonant component of absorption of much smaller amplitude. ^{4(a)}

Water vapor has absorption lines near 23 and 183 kMc/s and a large number of lines above 300 kMc/s. The wings of these submillimeter lines are the most important components of water vapor absorption in the microwave region except near the line center frequencies of 23 and 183 kMc/s. ^{4(b)}

The absorption of microwaves by atmospheric gases has received considerable attention in order that applications of these wavelengths when propagated in or through the earth's atmosphere can be evaluated. The results of many measurements have been reported. This paper is concerned with

absorption in the region of 125 kMc/s where there is a minimum of attenuation and a prospect of using this part of the spectrum for astronomical observations, communications, and radar.

The absorption coefficient of oxygen and water vapor as a function of frequency can be calculated using the Van Vleck-Weisskopf equation if the line intensity, the line center frequency, and the line width constant of each line are known. The intensity and center frequencies can be determined from theoretical calculations but are more accurately determined experimentally. Attempts to calculate the line width constant due to collision broadening for both oxygen and water vapor have not been too successful. An experimentally determined value is usually used for the line width constant and the constant is assumed to be the same for all unmeasured lines in calculations.^{4(c)} For the case of water vapor, only the 23 kMc/s and 183 kMc/s lines have been investigated experimentally, and the uncertainty in line width constant of the other submillimeter lines is often cited as the reason for disagreement between the experimental and calculated values of absorption.^{12(a)} Other disagreements in the value of absorption have also been noted that cannot be easily explained by this uncertainty in line width constant. The assumption has usually been made in these calculations that the absorption due to the two gases can be treated independently. While it is known that broadening by $\text{H}_2\text{O}-\text{H}_2\text{O}$ collisions would be greater than that of O_2-O_2 or O_2-N_2 collisions it has been thought that this effect would be small. Recent measurements indicate that it may be significant.⁵

II. SPECTROSCOPIC MEASUREMENTS AT MILLIMETER WAVELENGTHS

The measurement of the absorption of microwaves by gases requires a source of radiation and a scheme for detecting the radiation. The gas to be investigated may be contained in a length of waveguide, in a cavity or if atmospheric gases are being investigated, measurements may be made directly on the atmosphere.

Klystrons are commonly used as the source of radiation in spectroscopic measurements at microwave frequencies. Klystrons have a relatively monochromatic output, are electronically tuneable over a small frequency range and can be mechanically tuned over a relatively wide frequency range. Harmonics of the klystron output are used at the higher frequencies. They are obtained by exciting point-contact crystal diodes with the klystron output. ^{3(b)} Solar radiation has been used in some measurements on atmospheric gases.

Detection schemes for the shorter-wavelength microwaves are based on point-contact crystal diodes or bolometers. In video detection the crystals are excited by the microwave energy and the DC current through the crystal gives an indication of the power. In superheterodyne detection the incoming signal is mixed with local oscillator energy to give an output at an intermediate frequency which is the difference in frequencies of the input signal and the local oscillator. The operation of bolometers is based on the change in electrical conductivity of a small conductor when heated by the incoming energy. ^{3(c)}

Spectroscopic measurements at microwave frequencies require many other microwave and electronic components. Directional couplers, waveguide attenuators, waveguide transitions, antennas, electronic amplifiers, oscilloscopes and other conventional electronic equipment are used.

If the absorption line to be measured is of the order of a few megacycles in width the frequency of the source can be varied over a frequency interval several times the line width and the shape of the absorption line displayed. The frequency of the molecular line can also be varied by employing Stark or Zeeman modulation.

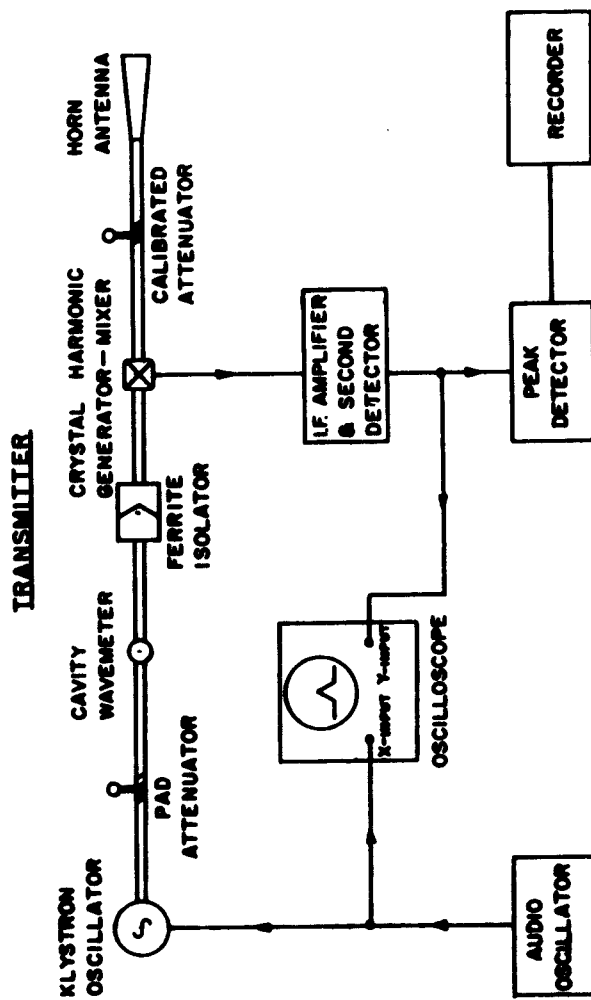
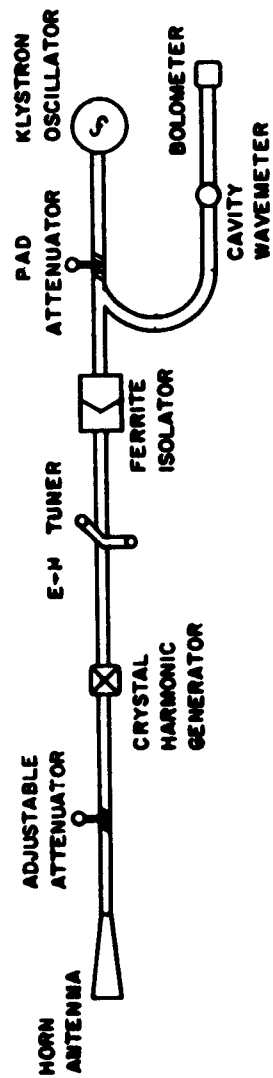
If measurements are to be made on gases at the higher pressures the absorption covers a band of frequencies many megacycles wide. Measurements must then be made at discrete frequencies. Most techniques involve the comparison of transmission over two paths although measurements employing cavities have been made. The variation in the Q of the cavity with different gases and at different frequencies is measured and the absorption determined.¹ One widely used method consists of transmitting the radiation down a waveguide or other enclosed transmission path where the molecular density can be controlled. With the guide evacuated, the gas to be measured can be introduced into the guide and the change in transmitted energy measured. If measurements are being made in the atmosphere, the change in the received energy level as the path length is changed is measured. Free space attenuation must be subtracted from the measured losses to determine the absorption losses.

III. INSTRUMENTATION

Two measurement techniques were used in gathering data for this report. Measurements were made by propagating through the atmosphere over several path lengths and by using an absorption cell. Since most of the transmitter and receiver equipment was common to both series of measurements, they will be described first. The transmitted signal was derived from a crystal harmonic generator driven by a reflex klystron. The receiver utilized crystal harmonic mixing to heterodyne the transmitted signal to an IF frequency of 30 megacycles.

A schematic of the transmitter and receiver is shown in Fig. 1. Figs. 2 and 3 are photographs of transmitter and receiver respectively.

The signal source in the transmitter and the local oscillator in the receiver consisted of Raytheon QK 864 klystrons driving Z225S crystals. These klystrons have a specified frequency range of 56 to 60 kMc/s although oscillation outside this range is often attained. An adjustable attenuator and ferrite isolator were inserted between each of the klystrons and crystals. The ferrite isolators were used to reduce the effect of load changes associated with the crystal harmonic mixer-generators from being reflected on the klystrons. The attenuators were used to adjust the klystron power to the crystal and to maintain a constant level of excitation at the various wavelengths at which measurements were made. On the transmitter an E-H tuner was also placed between klystron and crystal to improve impedance matching. The crystals



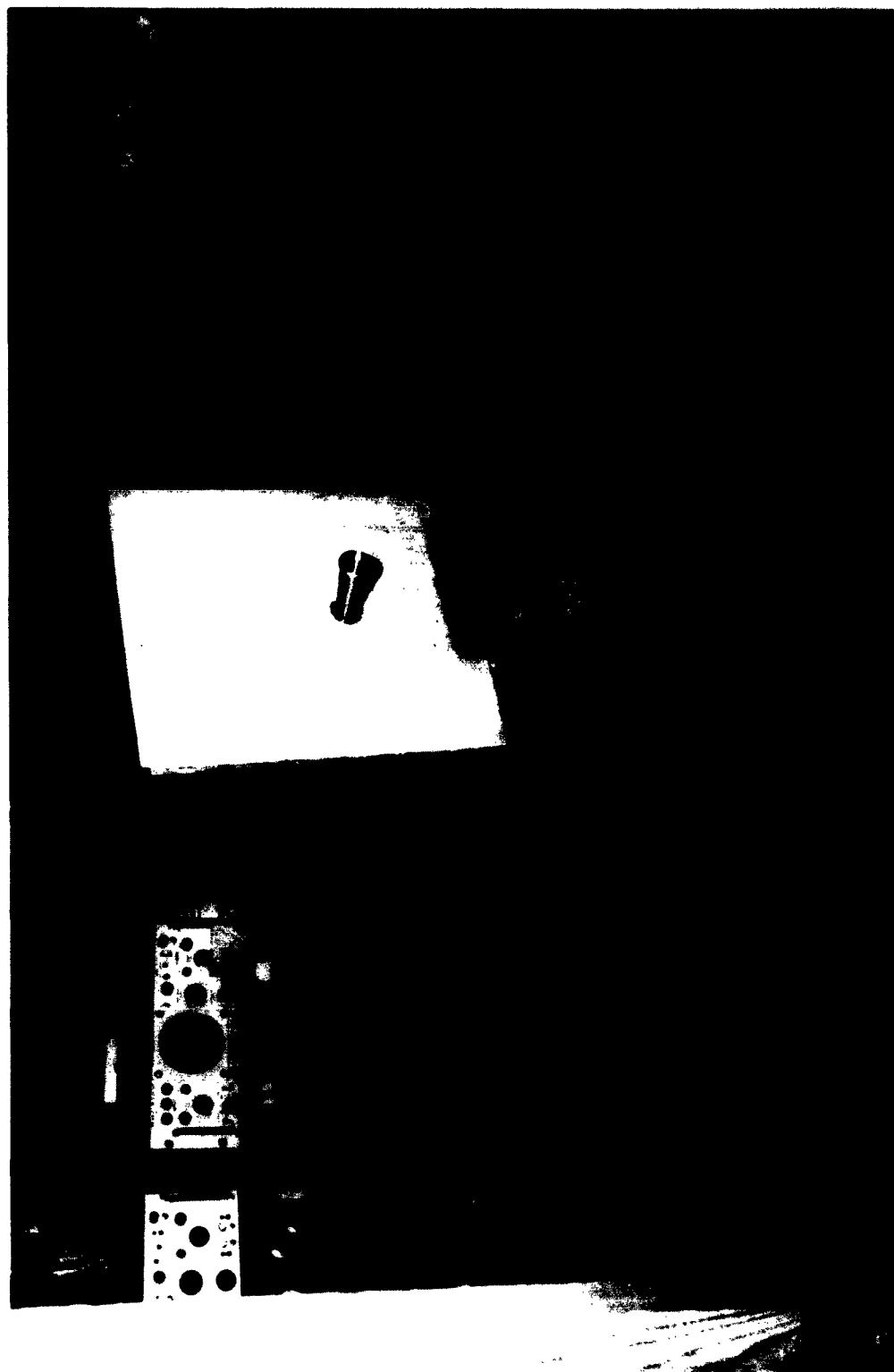
TRANSMITTER AND RECEIVER BLOCK DIAGRAM

FIG. 1.



PHOTOGRAPH OF TRANSMITTER.

FIG. 2.



PHOTOGRAPH OF RECEIVING EQUIPMENT.

FIG. 3.

were mounted in the waveguide with a connection for monitoring the DC current that resulted from the rectification of the high frequency signal. The crystal current gave an indication of the klystron output power level and, therefore, the harmonic power level at the crystals and allowed changes in power to be observed.

To permit the transmitted frequency to be determined, a directional coupler fed a part of the klystron output to a section of waveguide containing a cavity wavemeter and bolometer. The wavemeter was a Nardia Model M807 with a manufacturer specified accuracy of 0.02%. The receiver contained a similar wavemeter mounted between klystron and crystal.

The output of the transmitter crystal was fed through an adjustable pad attenuator to a horn antenna. A short waveguide filter in which the klystron fundamental frequency was below cutoff was also inserted between crystal and antenna to prevent any of the fundamental frequency energy from being radiated. A precision calibrated attenuator was located between a similar waveguide filter and antenna on the receiver to allow the recorded output from the receiver to be calibrated.

The intermediate frequency output of the receiver crystal harmonic generator-mixer was fed to the input of a narrow band 30 megacycle amplifier. Bias voltage adjustments on this amplifier permitted operations over a wide range of signal levels. The output of the IF amplifier was envelope detected in the second detector. Because of the difficulty in maintaining the frequencies

of the transmitter and the receiver local oscillator heterodyned within the pass-band of the IF amplifier the local oscillator klystron was frequency modulated by applying a sinusoidal signal to the reflector electrode. Thus the local oscillator was heterodyned at the IF frequency of 30 megacycles twice during each period of the modulation and an output of the IF pass-band obtained from the IF amplifier. The output of the second detector was then a series of pulses having the shape of the band pass of the IF amplifier.

For display purposes the output was fed to the vertical input of an oscilloscope with the modulation voltage applied to the horizontal input. The pulse displayed on the scope served as an easy means of determining the relative frequencies of the transmitter and local oscillator and the approximate signal amplitude.

The output of the second detector was also fed through several video amplifier stages to a peak detector circuit. The DC voltage output of the peak detector was supplied to a pen and ink strip chart recorder and, therefore, was a measure of the amplitude of the millimeter wavelength signal.

The calibrated attenuator mounted on the receiver was a DeMornay-Bonardi Model DB 410. This attenuator had a micrometer adjustment for varying the attenuation of the millimeter wavelength energy and was calibrated while installed in the receiver. Calibration of the attenuator was accomplished by assuming square-law dispersion of the transmitted signal. The distance between transmitter and receiver was varied in steps to give on-half decibel changes in signal at the receiver. The attenuator was adjusted to maintain

the same output recorder reading each time the spacing was changed and the attenuator micrometer readings were recorded. This procedure was repeated a number of times and the readings averaged. A plot of micrometer readings versus attenuation was made and served as the calibration curve for the attenuator.

Wide beam horns were mounted on the transmitter and receiver to minimize errors due to pointing over a 15 foot path.

IV. MEASUREMENT PROCEDURES

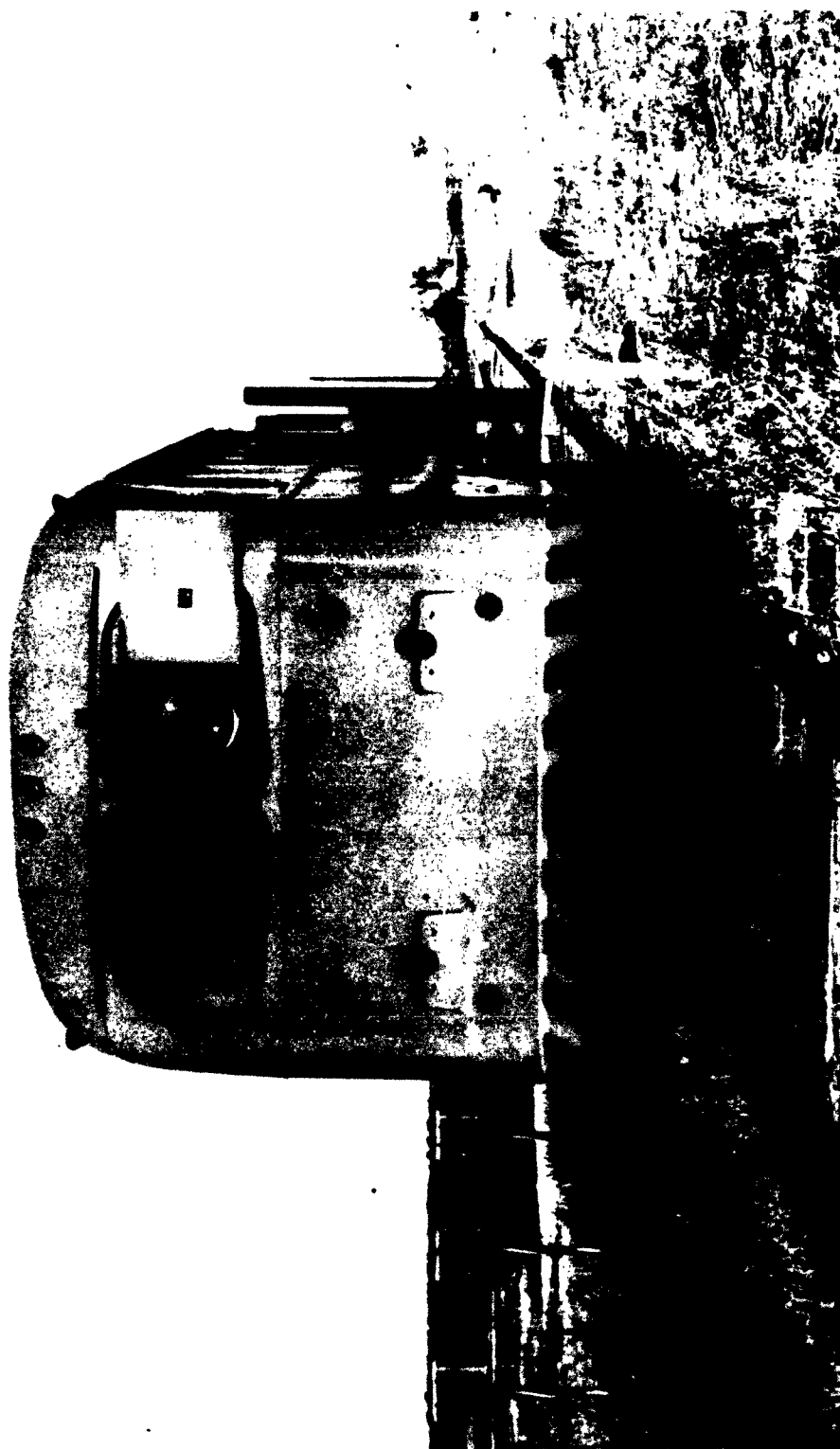
A. Atmospheric Measurements

Atmospheric measurements were made by propagating over path lengths of 210 ft., 420 ft., and 840 ft. and attributing all losses greater than free space dispersion losses to the atmospheric gases. Measured values of atmospheric loss were correlated with atmospheric water vapor density.

These measurements were made with the transmitter mounted 7 ft. above the ground in a bus which ran on a 1000 ft. length of railroad track. The receiver was stationed at one end of the track, 20 ft. above the ground. Three points, which corresponded to a spacing between the transmitter and receiver of 210, 420, and 840 ft., were marked off along the track. A photograph of the transmitting bus is shown in Fig. 4.

The eleven inch lense horn antennas were aligned with telescopic sights prior to each measurement. These antennas had a beamwidth of 0.65° at 120 kMc. and the 210 ft. separation was estimated to give operation in the far field.

The measurements consisted of a comparison of the received signal for 420 ft. and 840 ft. spacings of the transmitter and receiver. The output recorder reading was noted for a transmitter-receiver separation of 420 ft. and the calibrated attenuator on the receiver adjusted to give the same recorder reading for a transmitter-receiver spacing of 840 ft. The change in attenuator reading was then equal to the free space dispersion losses of six



PHOTOGRAPH OF TRANSMITTING BUS.

FIG. 4.

decibels plus the atmospheric loss over the 420 ft. difference in path lengths. To insure that the power output of the transmitter or the receiver gain had not changed the transmitter was returned to the 420 ft. point and the attenuator reset. If the second observation of the reference signal at the 420 ft. point deviated from the initial reference level by more than approximately 10% of the expected atmospheric losses, the data from the run was discarded.

In later measurements, the signal level for two each transmitter-receiver separations was compared. The change in signal between the 210 ft. to 420 ft. points was subtracted from the change in signal between the 420 ft. to 840 ft. points. This gave the atmospheric losses in a 210 ft. path length since the dispersion losses were the same for the two cases. The same precautions to check for equipment drift were used in these measurements. Sling psychrometer readings were taken to determine the atmospheric water vapor density.

Attenuation measurements through the atmosphere are desirable because they are made under the actual conditions that will be encountered in applications of this part of the radio spectrum. There were, however, a number of factors which hindered attempts to measure oxygen and water vapor attenuation.

In the technique described here, the six decibels of dispersion losses that were present greatly reduced the attainable accuracy. For example, if an absorption loss of 1 db/kilometer which corresponds to 0.128 db. in 420 ft., was to be measured with an accuracy of $\pm 10\%$, the system

was required to measure 6.128 ± 0.0128 db. in the 420 ft. path.

To move the transmitter from point to point, align the antennas and set the attenuator required about 20 minutes. This length of time created problems with drift of the klystrons, crystal harmonic generators, and other equipment. With the checks made for drift during each measurement a large number of the measurements were discarded.

Use of longer propagation paths would tend to decrease the effect of the 6 db. free space losses but the additional time required to take measurements and the limited power available at these frequencies would add to the difficulties.

B. Absorption Cell Measurements

Measurements of the difference in attenuation between dry air and outside atmospheric gases were made in a 500 ft. long 6 inch diameter copper pipe. The copper pipes absorption cell is shown in Fig. 5. The ends of the pipe were sealed with disks of teflon. The thickness of these dielectric windows was chosen experimentally for maximum transparency from the thicknesses available. The transmitter and receiver were fitted with 3 inch horn antennas. The distance between the horns and the ends of the cell was approximately 15 ft. Microwave absorber was placed around both ends of the cell to eliminate reflections from the surroundings. Pressure of the gas in the cell was measured with an absolute reading manometer.

Measurements of the attenuation of dry air and air-water vapor mixtures were made at five different pressures. These pressures



PHOTOGRAPH OF ABSORPTION CELL.

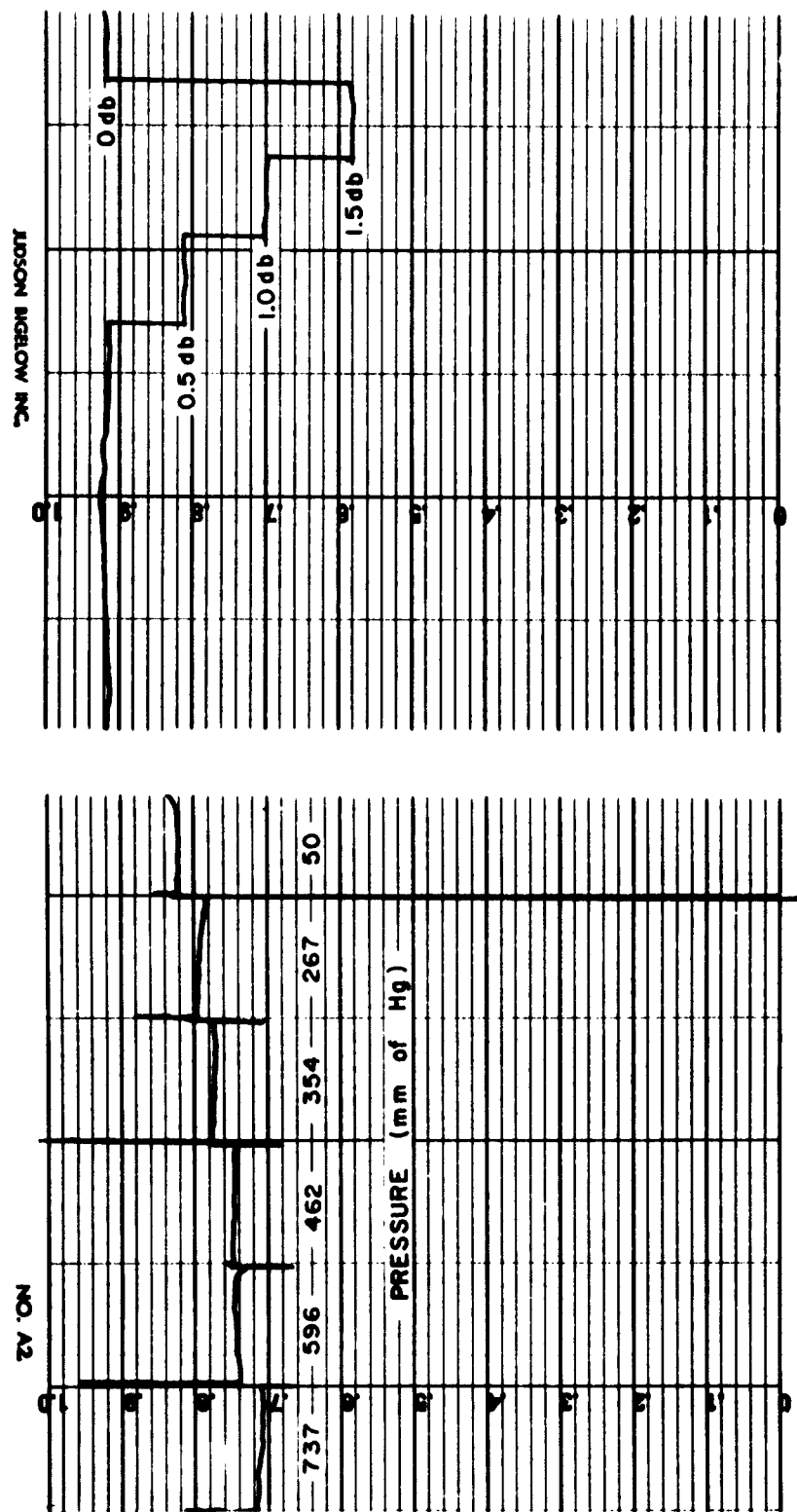
FIG. 5.

corresponded to the atmospheric pressure altitudes of 8, 6, 4, 2, and 0.25 kilometers as given by the U. S. Standard Atmosphere, 1962.¹⁰ Bottled dry air and outside air for which the water vapor content had been determined were used.

The attenuation was evaluated by using the signal level propagated down the cell at a gas pressure of 50 millimeters of mercury as a zero attenuation reference level. Air was added to bring the pressure up to 267 millimeters of mercury, the standard atmospheric pressure for 8 kilometers elevation, and the recorder run for about 30 seconds. This procedure was repeated for each pressure and the attenuation at each pressure was determined from the recorder strip. The scale on the recorder strip was calibrated by inserting attenuation in one-half db. steps with the calibrated attenuator. Typical calibration and data recordings are shown in Fig. 6.

Two thermometers, coated with heat conducting grease were attached near each end of the cell. The averaged readings of these thermometers was taken as representative of the air temperature in the cell.

The major problem associated with the absorption cell measurements was variations in the attenuation through the cell that were independent of the gas in the cell. These changes were due to movements of the dielectric windows with changes in absorption cell pressure. The deflection of the windows of approximately one inch over the range of gas pressures at which the measurements were made caused the transmission through the windows to change, thereby introducing an error into the measurements. These errors



CALIBRATION

DATA RUN

TYPICAL RECORDINGS.

FIG. 6.

were corrected by measurements of the attenuation in the absorption cell of helium, a non-resonant gas, over a pressure range similar to those used for dry air and outside air. Dry air was used to determine these errors at frequencies where its absorption is negligibly small.

Approximately 10 minutes were required to calibrate the receiver and make a run of data. Drift in the equipment over this period was another source of error. It was hoped that by taking a number of measurements and averaging, the error in the final results could be reduced.

V. RESULTS

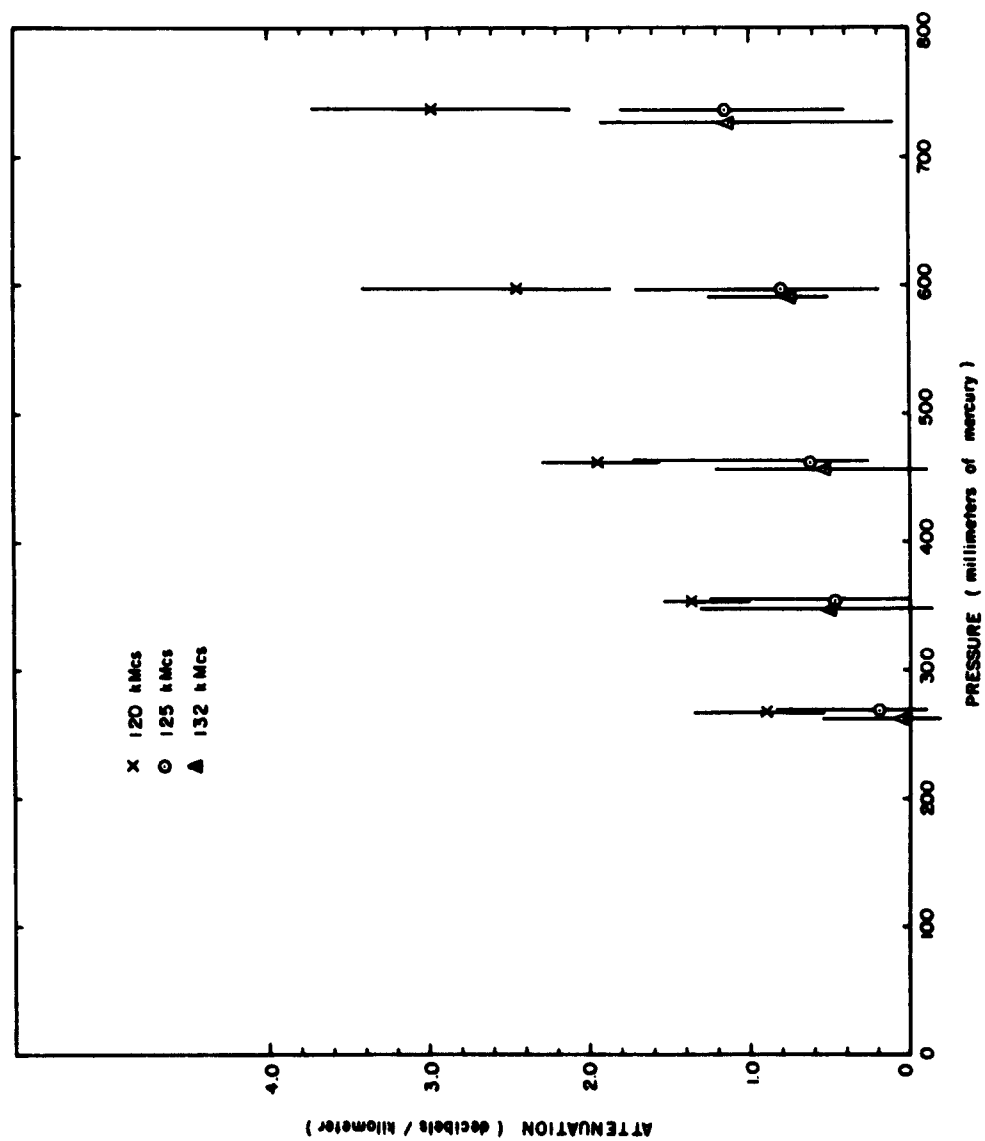
The results of the atmospheric measurements will not be reported because of the large uncertainties associated with them.

Attenuation measurements in the absorption cell of dry air and air-water vapor mixtures at five pressures were made at frequencies of 120, 125 and 132 kMc/s. These measurements were made over a period of five weeks during which the water vapor density in the atmosphere varied from 13 to 19.9 grams per cubic meter and the absorption cell temperature varied from 23.2° C to 55.3° C.

The measured values of attenuation were adjusted to correspond to a temperature of 300° Kelvin by multiplying them by $(T/300)^3$, where T was the temperature of the absorption cell in degrees Kelvin.

The errors due to movements of the dielectric windows on the absorption cell were evaluated by measurements with helium at 120 kMc/s. At 125 and 132 kMc/s the attenuation of dry air is small and dry air runs were used to determine these errors.

Since the mean water vapor density of the atmosphere during the period of measurements corresponded to an atmosphere with approximately 2% water vapor molecules, the measured values of attenuation plotted versus pressure in Fig. 7 were adjusted to a common water vapor molecular density of 2% by assuming the attenuation is directly proportional to water vapor density. The range of values observed, indicated by the vertical line through each point, is



MEASURED VALUES OF ATMOSPHERIC ATTENUATION VS.
PRESSURE FOR 2% WATER VAPOR MOLECULAR DENSITY

FIG. 7.

largely attributed to measurement uncertainties.

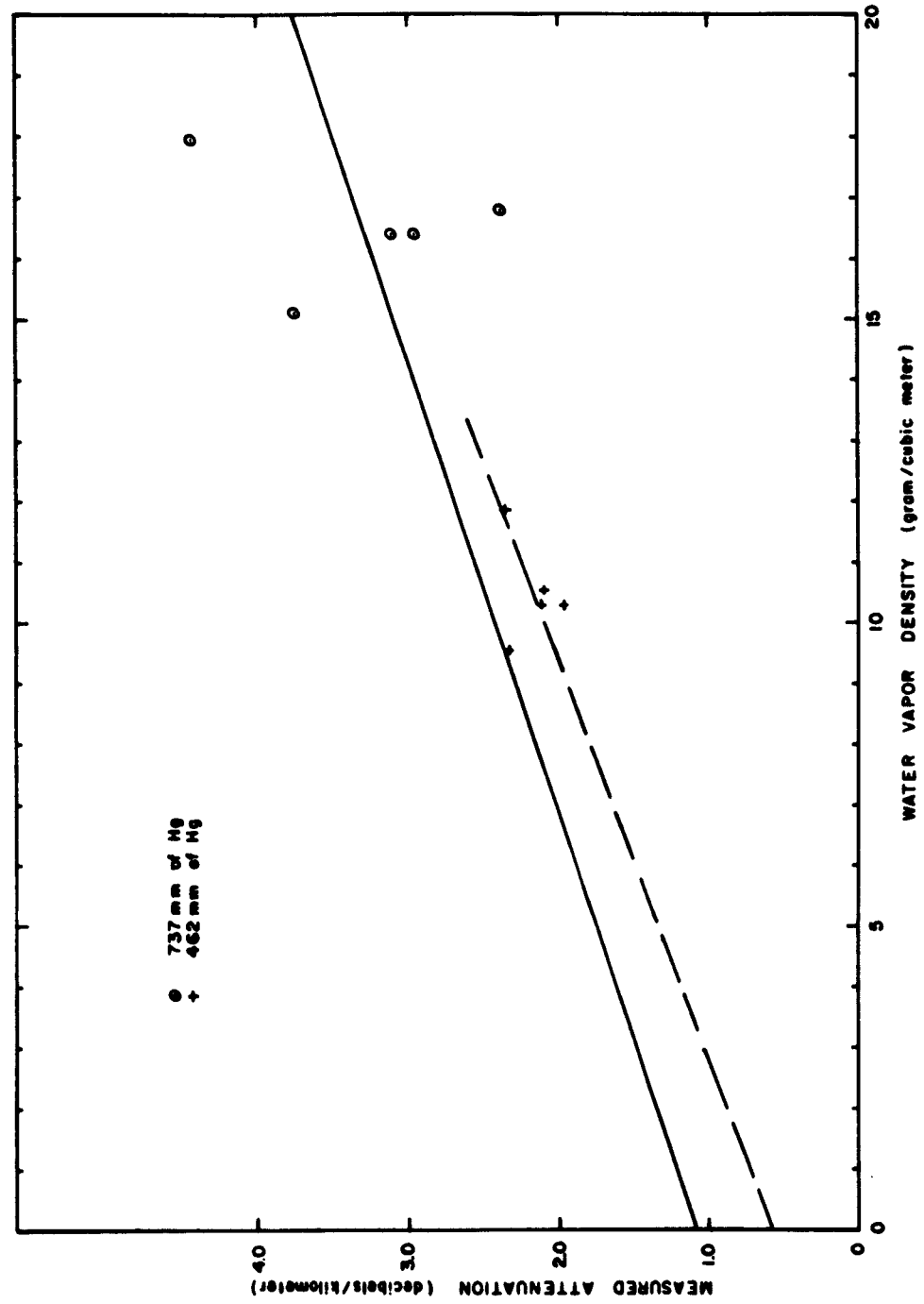
Figs. 8, 9, and 10 are plots of the measured values of attenuation versus water vapor density, adjusted to 300° K, at the frequencies of 120, 125, and 132 kMc/s, respectively. The attenuation at pressures of 267 and 730 millimeters of mercury are typical of those observed. A straight line variation of attenuation versus water vapor was assumed since the range of water vapor encountered during measurements did not permit the exact relation between water vapor density and attenuation to be determined. Straight lines are shown in Figs. 8, 9, and 10 drawn through dry air attenuation values at the y-axis intercept and the average point of the air-water vapor measurements.

Fig. 11 is a plot of the average dry air attenuation measured at 120 kMc/s versus pressure. The curve drawn on this figure is the attenuation calculated by assuming an oxygen line with a center frequency of 118.75 kMc/s a half width of 1.35 kMc/s and a peak attenuation of 1.7 decibels per kilometers at sea level pressure.

The water vapor sensitive losses were determined by correlating the difference in the observed attenuation of dry air and outside air with measurements of the water vapor density in the outside air. The average values of the water sensitive losses plotted versus pressure for each frequency are shown in Fig. 12. Since the average water vapor density was slightly different for the measurements at each frequency, the values plotted in Fig. 12 were obtained by adjusting the average values measured to correspond to an atmosphere with 2% water vapor molecules to allow direct comparison of the

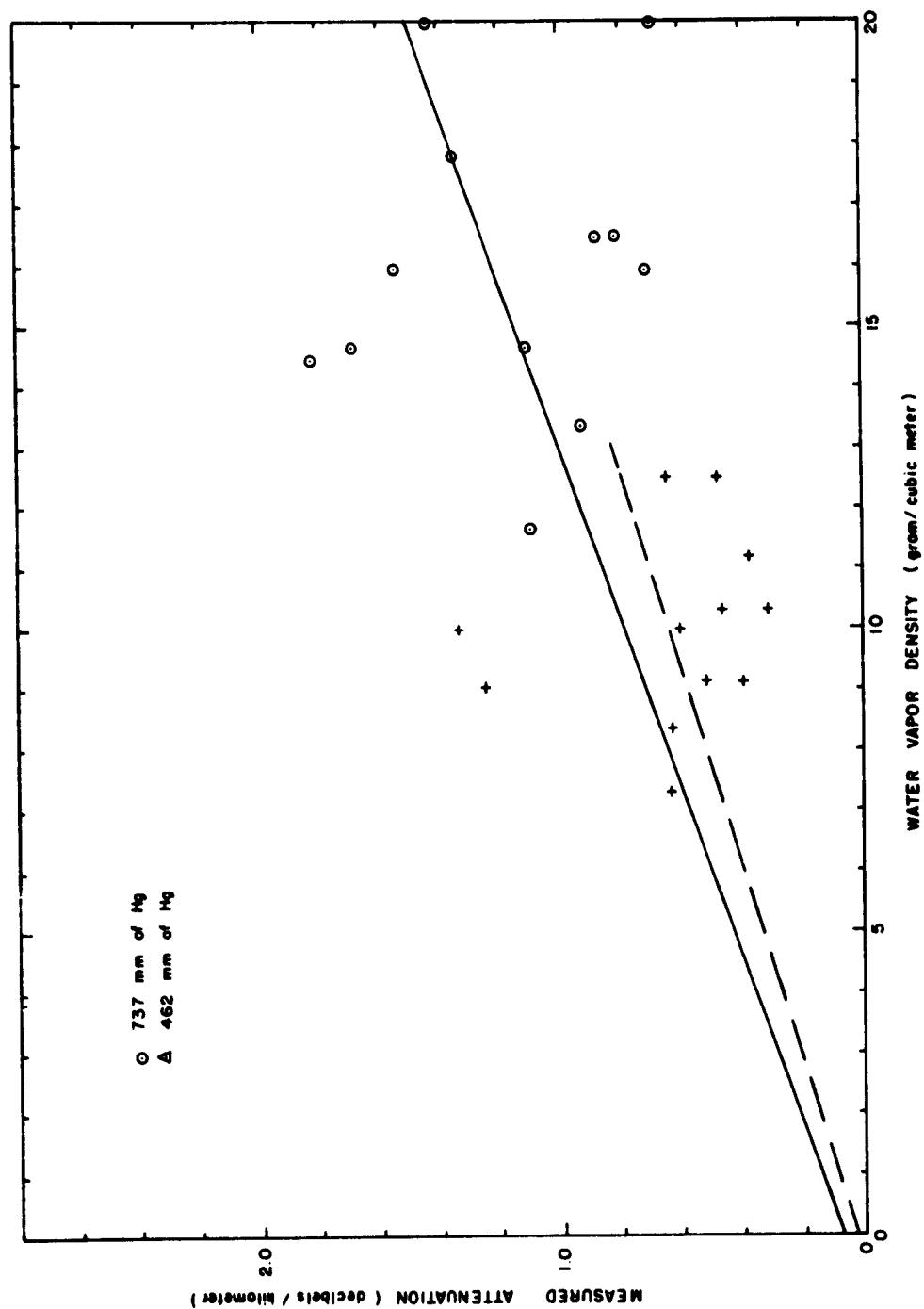
attenuation at the three frequencies.

In Fig. 13, the measured water vapor attenuation per unit water vapor density is plotted versus pressure for each frequency. These values were obtained by dividing the average attenuation measured by the average water vapor density at each pressure and frequency.



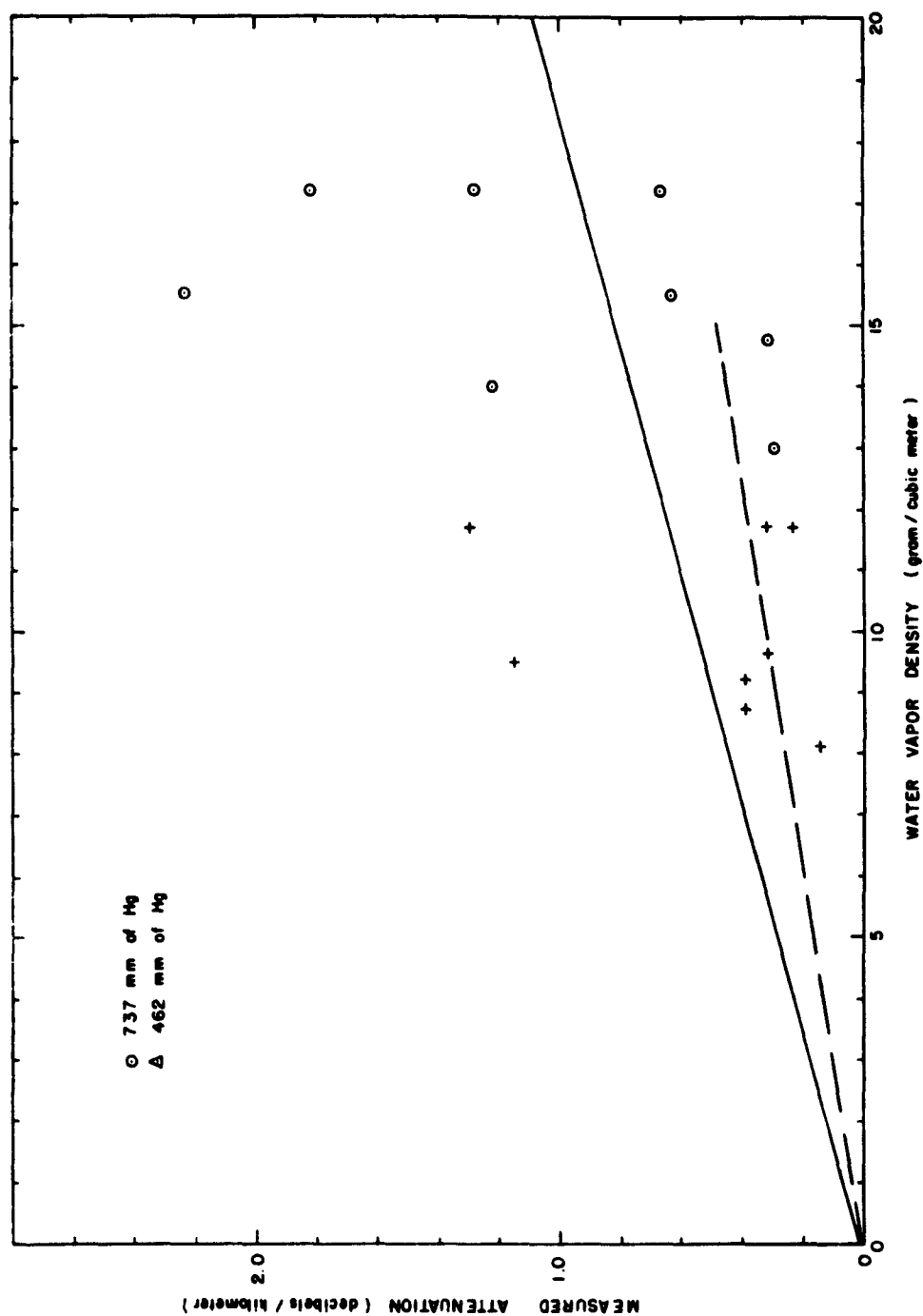
ATTENUATION VS. WATER VAPOR DENSITY AT 120 KMcS FOR PRESSURES OF 737 AND 462 MILLIMETERS OF MERCURY.

FIG. 8.



ATTENUATION VS WATER VAPOR DENSITY AT 125 KMcS FOR
PRESSURES OF 737 AND 462 MILLIMETERS OF MERCURY

FIG. 9.



ATTENUATION VS. WATER VAPOR DENSITY AT 132 KMcS FOR
PRESSURES OF 737 AND 462 MILLIMETERS OF MERCURY

FIG. 10.

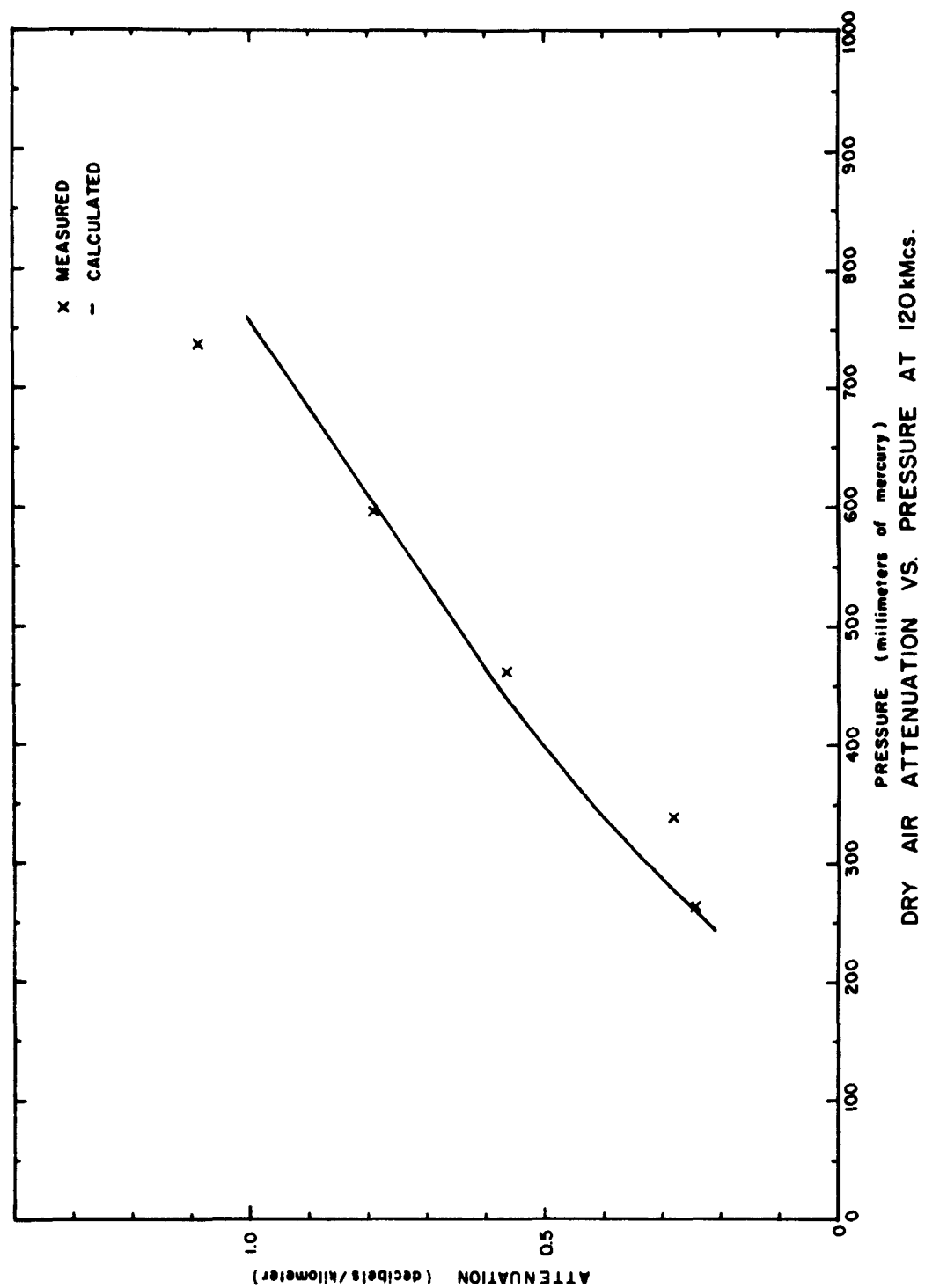
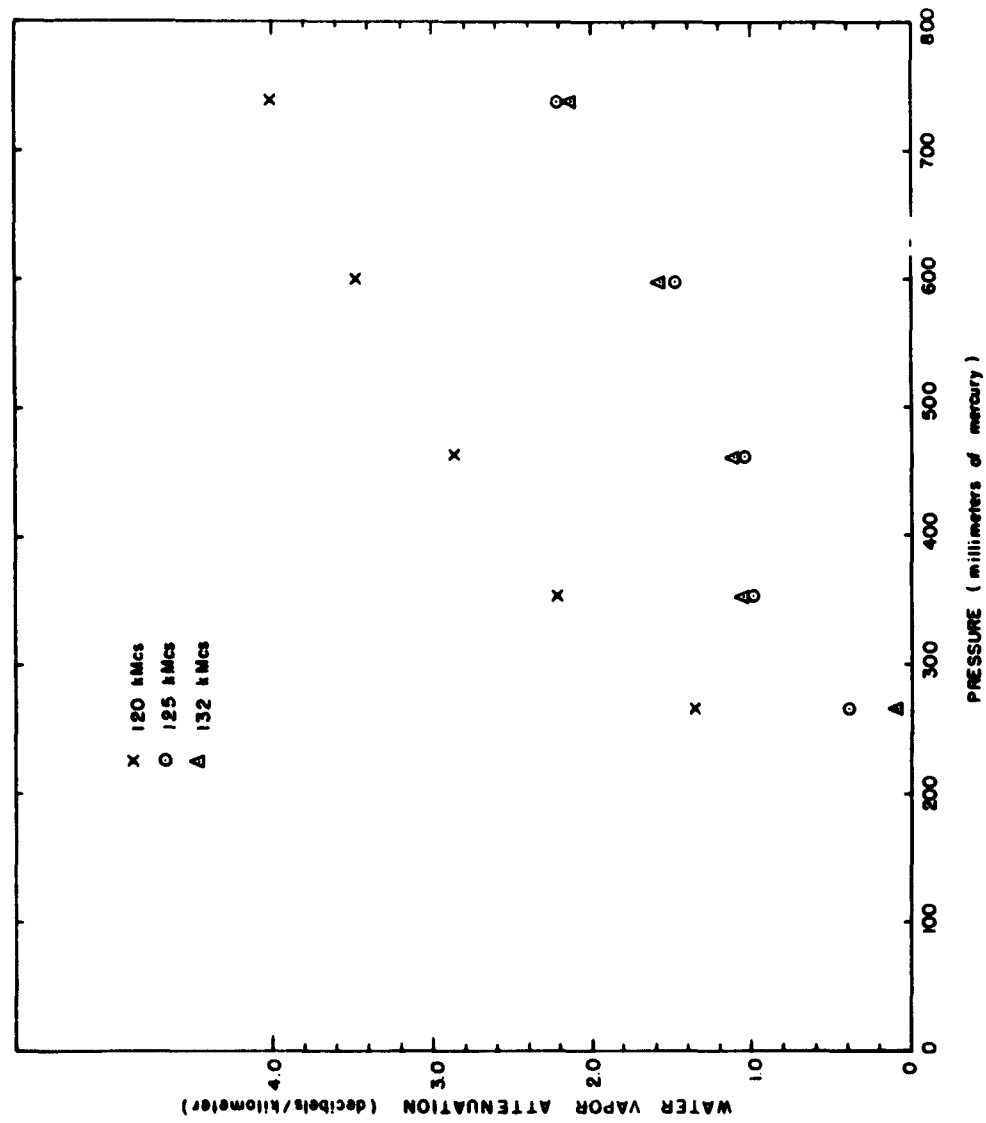
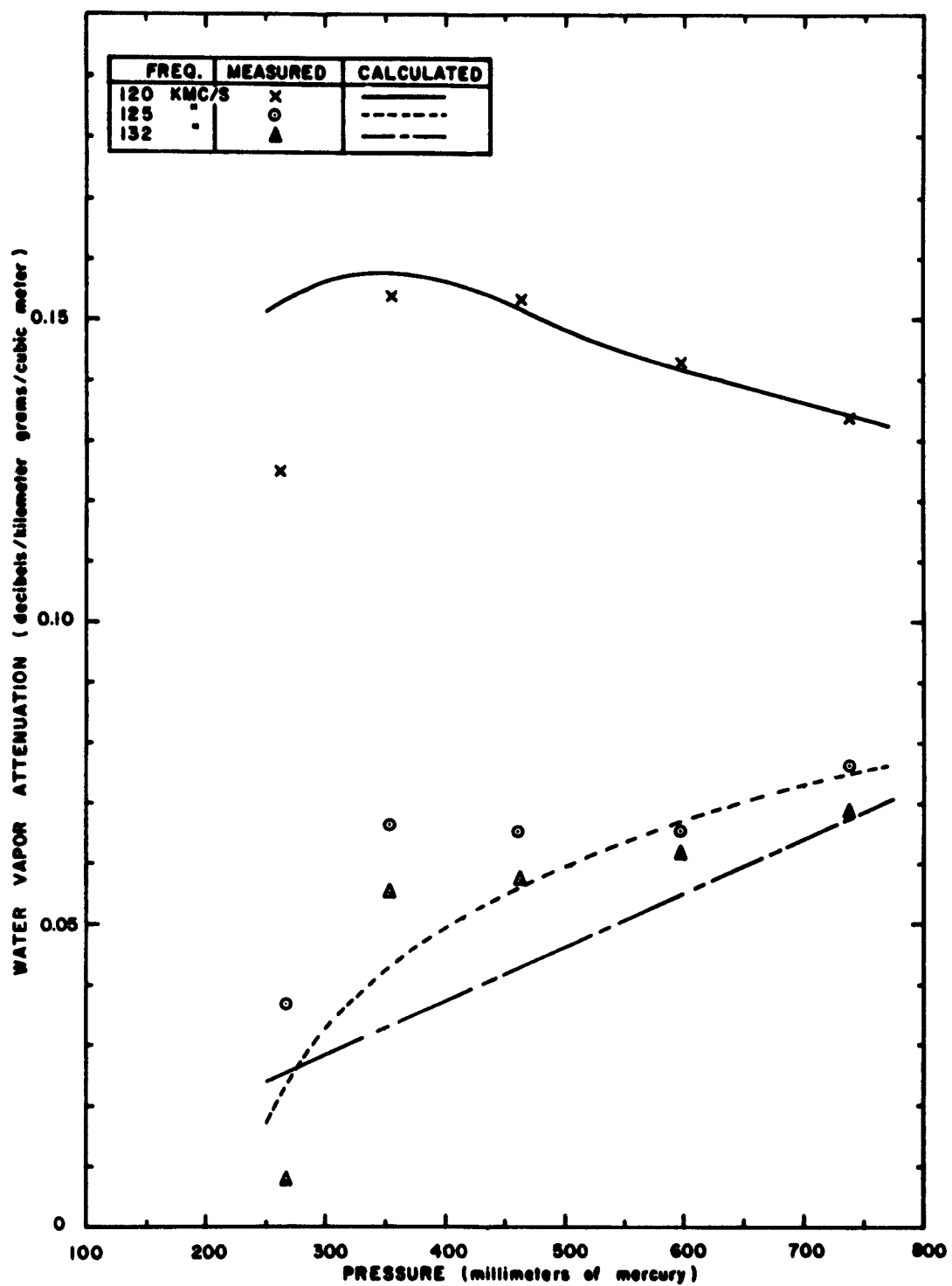


FIG. 11.



WATER VAPOR ATTENUATION VS. PRESSURE FOR 2% WATER VAPOR
MOLECULAR DENSITY.

FIG. 12.



WATER VAPOR ATTENUATION VS. PRESSURE FOR A CONSTANT
WATER VAPOR DENSITY OF ONE GRAM PER CUBIC METER.

FIG. 13.

VI. DISCUSSION

From Fig. 13, a discrepancy between these measurements and the attenuation predicted by theory is apparent. Current water vapor absorption theory predicts no absorption lines in the frequency region of these measurements. The attenuation in this region is theoretically attributable to the wings of the water vapor line near 23 kMc/s and the numerous lines above 180 kMc/s. This residual attenuation per unit water vapor density is proportional to the half-line, half-width of the water vapor lines and is, therefore, approximately proportional to pressure. Water vapor absorption theory also predicts that attenuation increases monotonically with increasing frequency in this frequency region. From Fig. 13, it is seen that the measured pressure and frequency dependence of absorption does not agree with these predictions.

A number of measurements at atmospheric pressure in the 35 to 140 kMc/s frequency region have been reported by the Electrical Engineering Research Laboratory of The University of Texas and others. These measurements have yielded values of attenuation consistently larger than predicted by calculations based on a half-line, half-width of 0.1 cm^{-1} for the water molecule. Also decreases in attenuation with increasing frequency have been observed in the regions near oxygen absorption lines. Several possible explanations for these anomalies have been proposed. The possibility that the effect of the presence of water vapor on the line-width of oxygen absorption lines is much greater than expected and the existence of unpredicted water vapor lines have been considered.^{8(b)} However, the measurements that had

been made did not permit definite conclusions to be made about the cause of these irregularities.

According to collisional theories of line broadening, the line width parameter for a mixture of two gases is given by ^{3(d)}

$$\Delta \nu \propto p_a \frac{\bar{v}_a \sigma_a}{2\pi} + p_b \frac{\bar{v}_b \sigma_b}{2\pi}$$

where the subscripts a and b refer to gases a and b

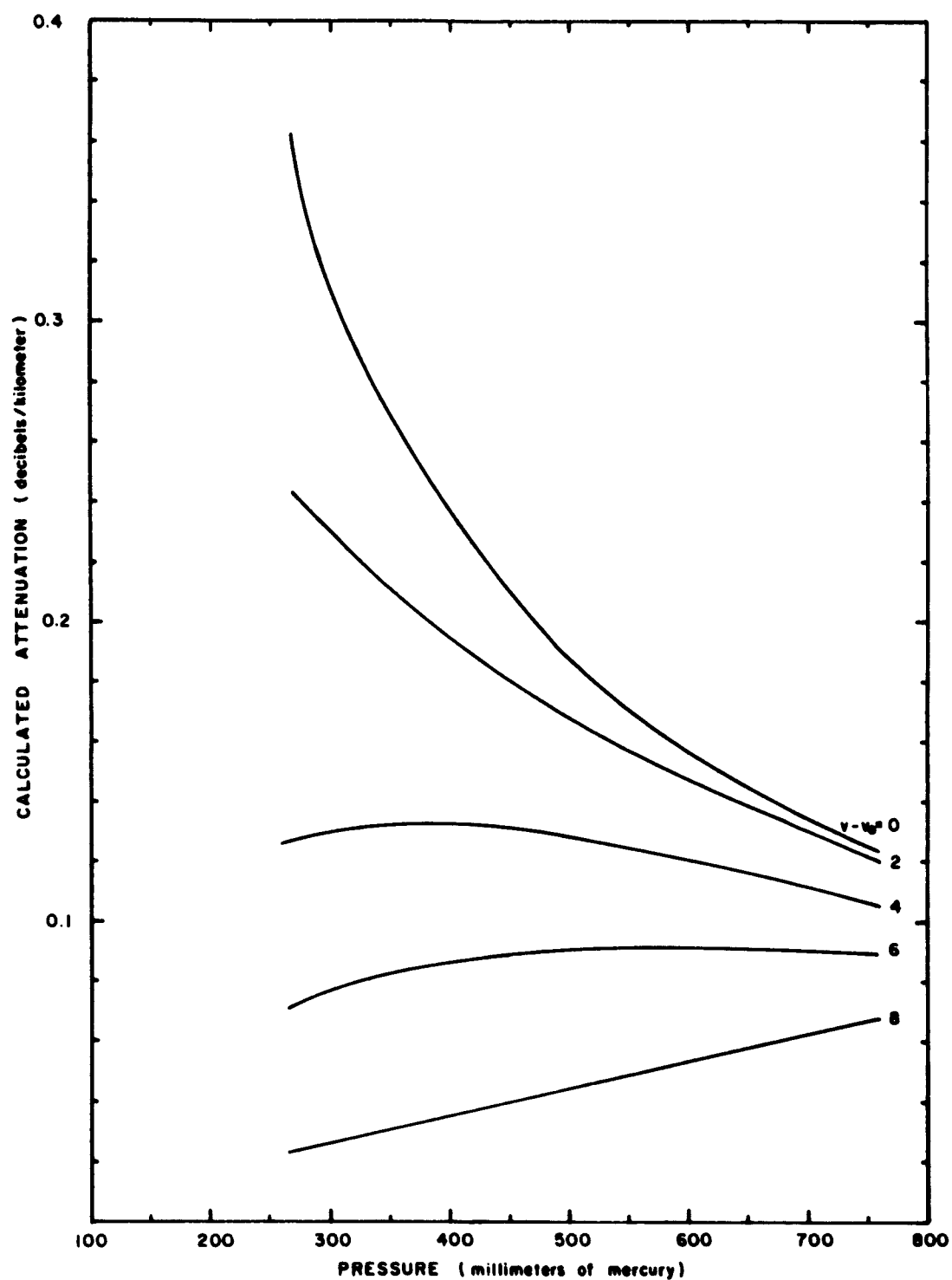
p is the partial pressure of the gas

\bar{v} is the average molecular velocity of the gas molecules

σ is the collision cross section of the gas molecules

For the measurements reported in this thesis the ratio of the partial pressures of dry air and water vapor was constant for each data run. The $\Delta \nu$ should have been proportional to total pressure regardless of the relative collision cross sections of the various gas molecules and the discrepancy noted in Fig. 13 could not have been caused by a water vapor density dependence of either oxygen or water vapor line widths.

In Fig. 14, the attenuation per unit water vapor density is plotted versus pressure for several frequencies near a water vapor absorption line. These curves were calculated from the Van Vleck-Weisskopf equation assuming $\Delta \nu$ is proportional to pressure. Comparison of the calculated curves in Fig. 14 with the measured pressure dependence of attenuation in Fig. 13 indicated that a water vapor line may exist in this frequency region.



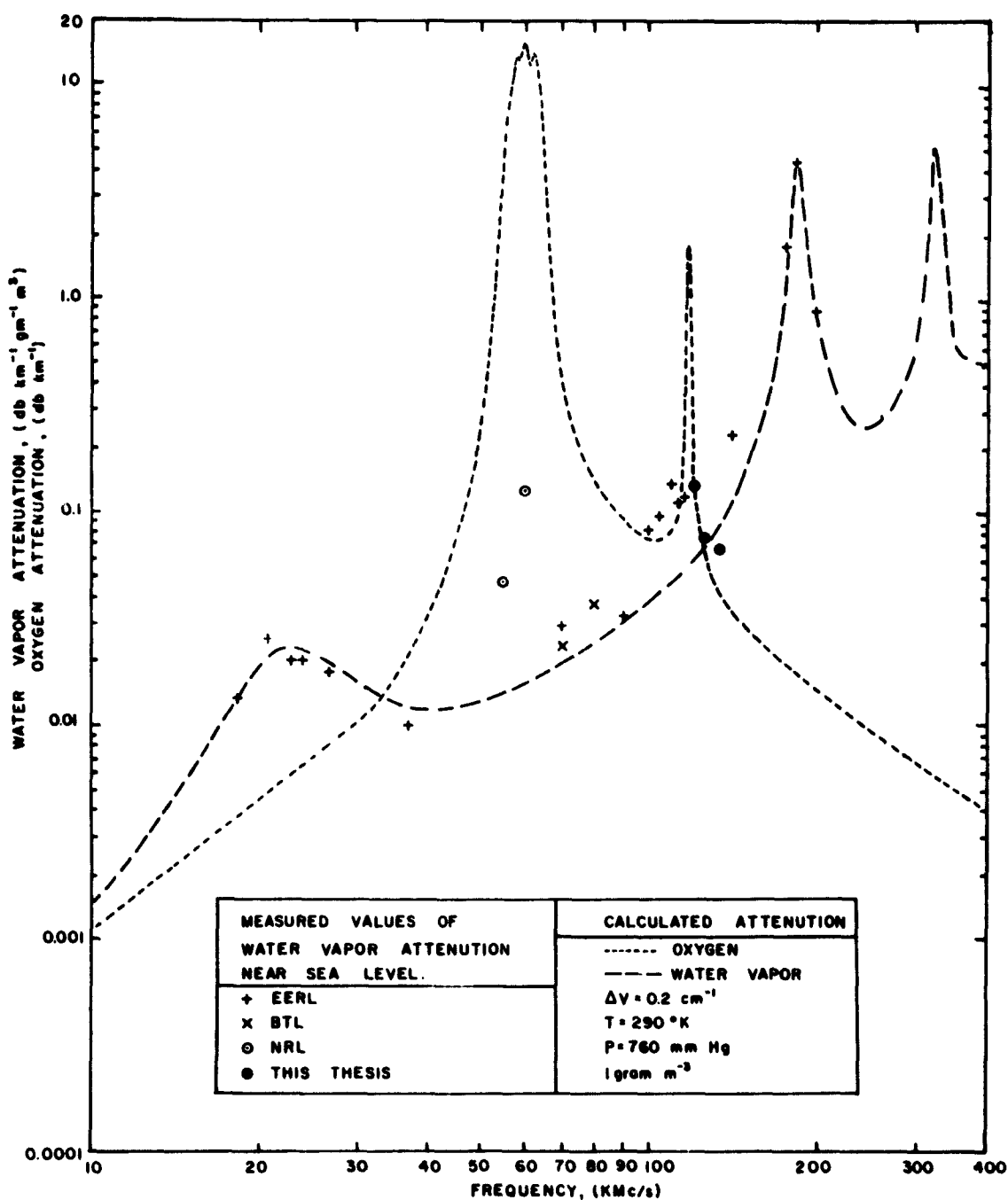
CALCULATED ATTENUATION VS. PRESSURE FOR CONSTANT
MOLECULAR DENSITY IN THE REGION OF AN ABSORPTION
LINE.

FIG. 14.

The presence of a water vapor line near 121 kMc/s describes the measured data. The curves drawn in Fig. 13 were calculated assuming a water vapor line with center frequency 121.0 kmc, half-width of 2.7 kMc/s and peak intensity of $0.107 \text{ db/Km gm/m}^3$ at sea level pressure and a residual attenuation of 0.040, 0.046 and $0.063 \text{ db/Km gm/m}^3$ at 120, 125, and 132 kMc/s respectively.

Previous measurements of water vapor attenuation made by Electrical Engineering Research Laboratory (EERL), Bell Telephone Laboratories (BTL) and the Naval Research Laboratory (NRL)⁸ are shown in Fig. 15 along with the measurements reported here. Calculated curves for the attenuation of oxygen and water vapor are also shown in Fig. 15. Peaks in attenuation can be seen near 60, 80, and 110 kMc/s

This previous data, when considered with the data reported here adds significance to the conclusion that a number of relatively weak water vapor absorption lines exist in the region between the 23 and 183 kMc/s lines.



MEASURED VALUES OF WATER VAPOR ATTENUATION AND CALCULATED OXYGEN AND WATER VAPOR ATTENUATION.

FIG. 15.

VII. CONCLUSIONS

The measurements reported in this thesis indicate the existence of a water vapor absorption line centered near 121 kMc/s with half-intensity half-width of 2.7 kMc/s and peak intensity 0.107 db/km gm/m³ at sea level pressure. These results also indicate that the anomalous values of water vapor absorption observed previously are the result of unpredicted water vapor absorption lines and are not due to excessive broadening of oxygen absorption lines by the presence of water vapor.

BIBLIOGRAPHY

1. Becker, G. E., and L. H. Autler, "Water Vapor Absorption of Electromagnetic Radiation in the Centimeter Wavelength Range," Physical Review, Vol. 70, pp. 300-307, September, 1946.
2. Coats, G. T., R. A. Bond, and C. W. Tolbert, "Propagation Measurements in the Vicinity of the 183 Gc/s Water Vapor Line," The University of Texas, Electrical Engineering Research Laboratory, Report No. 7-20, February 5, 1963.
3. Gordy, W., W. V. Smith, and R. F. Tramborulo, Microwave Spectroscopy, Wiley and Sons, New York, 1953. a) p. 189, b) p. 45-46, c) pp. 34-37, d) p. 192.
4. Straiton, A. W., and C. W. Tolbert, "Anomalies in the Absorption of Radio Waves by Atmospheric Gases," Proceedings of the Institute of Radio Engineers, Vol. 48, pp. 898-903, May 1960. a) p. 898, b) p. 900, c) p. 898-899.
5. Straiton, A. W., and C. W. Tolbert, "An Analysis of Recent Measurements of the Atmospheric Absorption of Millimeter Radio Waves," Proceedings of the Institute of Radio Engineers, Vol. 49, pp. 649-650, March 1961, p. 650.
6. Schulze, A. E., "A Spectroscopic Measurement of the Resonant Absorption of Microwave Energy by Oxygen in the 2.5 Millimeter Wavelength Region," Master's Thesis, The University of Texas, August, 1963.
7. Tolbert, C. W., C. O. Britt, and J. H. Douglas, "Radio Propagation Measurements in the 100 to 118 kMc/s Spectrum," The University of Texas, Electrical Engineering Research Laboratory, Report No. 107, April 15, 1959.
8. Tolbert, C. W., A. W. Straiton, and J. R. Gerhardt, "A Study and Analysis of Anomalous Atmospheric Water Vapor Absorption of Millimeter Wavelength Radiation," The University of Texas, Electrical Engineering Research Laboratory, Report No. 117, October 31, 1960. a) pp. 2-3, b) pp. 14-18.
9. Townes, C. H., and A. L. Schawlow, Microwave Spectroscopy, McGraw-Hill Book Company, New York, 1951. a) p. 2, b) p. 19, c) pp. 336-337, d) p. 373.

10. U. S. Standard Atmosphere, 1962, Washington, D. C., 1962, pp. 37-53.
11. Van Vleck, J. H., "The Absorption of Microwaves by Oxygen," Physical Review, Vol. 71, pp. 413-424, April, 1947.
12. Van Vleck, J. H., "The Absorption of Microwaves by Uncondensed Water Vapor," Physical Review, Vol. 71, pp. 425-433, April 1, 1947.
13. Van Vleck, J. H., and V. F. Weisskopf, "On the Shape of Collision Broadened Lines," Reviews of Modern Physics, Vol. 17, pp. 227, 1945.
14. Wilson, E. B., J. C. Decuis, and P. C. Cross, Molecular Vibrations, McGraw-Hill Book Company, 1955, p. 6.

AF 33(657)-8716

DISTRIBUTION LIST

	Attn:	No. copies
Defense Documentation Center Cameron Station Alexandria, Virginia - 22314		10
Hq., AFSC Andrews Air Force Base Washington 25, D.C.	SCTAE/Col. Schulte	1
Electronics Systems Division L. G. Hanscom Field Bedford, Mass.	ESRDE/Maj. John Hobson	1
Aeronautical Systems Division Wright-Patterson AFB, Ohio	ASRNCF-2	4 + 1 reprod.
	ASRNCF/Mr. Hill	1
	ASRNC/Mr. Stimmel	1
	ASRNG/Mr. R. J. Doran	1
	ASRNGE-2/Mr. Wm Harmon	1
	ASRNR, Mr. E. B. Woodford	1
	ASAPRL/Tech Doc Library	1
	ASRNCS-1/Mr. Bartlett	1
	ASRNE/Mr. Noble	1
	ASRNRS-4/Mr. Schoonover	1
Air Force Cambridge Research Laboratories Electronics Research Directorate L. G. Hanscom Field Bedford, Mass.		1
Air University Maxwell AFB, Alabama	Library 7575	1
U. S. Naval Research Laboratory Washington 25, D.C.	Library	1
U. S. Army Signal Research and Development Laboratory Fort Monmouth, New Jersey	Technical Reports Library	1
Commanding Officer Harry Diamond Laboratories Washington 25, D.C.	Library	1
Commanding Officer U. S. Army Electronics Research and Development Activity White Sands Missile Range, New Mexico - 88002	SELWS-M, Chas. Querfeld	1
Collins Radio Company Cedar Rapids, Iowa	Mr. G. Phillips	1
Lincoln Laboratory, M. I. T. P. O. Box 73 Lexington 73, Mass.	Documents Library	1